



Effect of calcination temperature on B-site vacancy content of $\text{La}_{0.75}\text{Sr}_{0.25}\text{Mn}_{0.92}\Delta_{0.08}\text{O}_{3-\delta}$ perovskite[☆]

Denghui Ji^{a, b}, Shuling Wang^{c, *}, Xingze Ge^d, Xinju Xiao^{a, b}, Liwei Wang^{a, b}, Zhiwei Zeng^{a, b}, Congmin Zhang^{a, b}

^a School of Electrical Engineering, Liupanshui Normal University, Liupanshui 553004, China

^b The Key Laboratory of Opto-electronic Information Technology of Liupanshui City, Liupanshui 553004, China

^c School of Science of Hebei University of Engineering, Hebei University of Engineering, Handan 056038, China

^d Ceramic Science Institute, China Building Materials of Academy, Beijing 100024, China

ARTICLE INFO

Article history:

Received 22 March 2017

Received in revised form

27 May 2017

Accepted 31 May 2017

Available online 18 August 2017

Keywords:

Lanthanum manganite

TEM

B-site vacancy

Core–shell model

Rietveld fitting technique

Rare earths

ABSTRACT

Lanthanum manganite with cation vacancies from nominal $\text{La}_{0.75}\text{Sr}_{0.25}\text{Mn}_{0.92}\Delta_{0.08}\text{O}_{3-\delta}$ nanocrystalline powder was successfully prepared at different calcination temperatures using the sol–gel method. X-ray diffraction shows that as the calcination temperature (T_{Cal}) increases, the crystal particle diameter increases, but the B-site vacancy content decreases. According to a powder diffraction profile fitting technique and transmission electron microscopy results, the vacancy content can be estimated as 0.08, 0.01, and 0.005 for $T_{\text{Cal}} = 1073, 1273, \text{ and } 1473 \text{ K}$, respectively. Magnetization versus temperature curves show that the magnetic transition temperatures, including the Curie temperature, are influenced by both B-site vacancies and double-exchange interaction between Mn^{3+} and Mn^{4+} cations. A core–shell model is proposed for vacancies located on the surfaces of the crystal particles. As an application, the magnetic moment angle θ_{ij} between Mn^{3+} and Mn^{4+} cations on the surface, which decreases with decreasing vacancy content, can be obtained.

© 2018 Chinese Society of Rare Earths. Published by Elsevier B.V. All rights reserved.

1. Introduction

ABO₃-type perovskites such as $\text{Ln}_{1-x}\text{M}_x\text{MnO}_3$ (where Ln is a trivalent rare earth element, and M is a trivalent rare earth or divalent alkali earth element) have received much attention owing to their useful physical properties such as the double-exchange interaction,¹ the Jahn–Teller effect,² and giant magnetoresistance,³ and potential application in materials such as catalysts,^{4,5} electrolytes in fuel cells,⁶ thermochemical energy storage media,⁷ microwave absorption materials,⁸ and perovskite solar cells.^{9–11}

The valence state and ionic radius of the doped cation at the A-sites induce the change of the valence of the Mn cations at the B-site, and cause lattice distortion, and result in the physical

properties. The Ag-doped manganite powder samples $\text{La}_{0.7}\text{Sr}_{0.1}\text{Ag}_x\text{MnO}_{3-\delta}$ synthesized by Hou et al indicates the variations of the specific saturation magnetizations at 300 K and the Curie temperatures.¹² $\text{La}_{0.9}\text{Sn}_{0.1}\text{MnO}_{3+\delta}$ thin films epitaxially grown on single-crystal substrates by pulsed-laser deposition was found that the maximum magnetoresistance ratio was 10³% at 233 K and 6 T.¹³ The spatial fluctuation of the magnetic domain and charge/orbital ordering structure at around the Curie temperature exhibited a colossal magnetoresistance in compound $\text{La}_{0.69}\text{Ca}_{0.31}\text{MnO}_3$.¹⁴ However, the most distinctive member of the doped cation at the A-sites is the self-doping (A-sites vacancy).

Studies focused on self-doping in perovskite compounds^{15–17} have all assumed that vacancies exist only at A sites and that the vacancy content is related to the self-doping level x . However, these works disagree with the dependence of the Curie temperature T_C on the Mn^{4+} ion content at B sites, and a physical model¹⁸ was proposed for the vacancy distribution in $\text{Ln}_{1-x}\text{M}_x\text{MnO}_3$ (here, Ln is a rare earth ion, and M is an alkaline earth ion) based on the thermal equilibrium theory of crystal defects. First, because the available space at B sites is smaller than that at A sites, vacancies should appear at B sites instead of A sites in the ABO₃ self-doped

[☆] **Foundation item:** Project supported by the National Natural Science Foundation of China (11504078), the Key Project of the Education Department of Guizhou Province (KY2015379), Joint Funds of Department of Science and Technology of Guizhou Province, Liupanshui Administration of Science and Technology and Liupanshui Normal University (LH[2014]7449, LH[2014]7456), and Research Foundation for Advanced Talents of Liupanshui Normal University (LPSSYKYJJ201404).

* Corresponding author.

E-mail address: shuling2015@hebeu.edu.cn (S.L. Wang).

manganite $\text{La}_{1-x}\text{MnO}_{3-\delta}$. Second, the main source of vacancies in the samples is the preparation method rather than the self-doping level. In our earlier study,¹⁹ it has been found that B-site vacancies have an important effect on the structural and magnetic properties of a series of sample perovskites, $\text{La}_{0.75}\text{Sr}_{0.25}\text{Mn}_{1-x}\text{O}_{3-\delta}$ ($x = 0.00, 0.03, 0.05, 0.08, 0.10, 0.13, 0.15, \text{ and } 0.17$). It was found that the B-site vacancy content has a maximum value z_m (0.08) at a calcination temperature T_{cal} of 1073 K, because the samples with $x \leq 0.08$ have a single perovskite phase, and the number of lattice points at A sites is equal to that at B sites. However, there are no reports on how the maximum value of the B-site vacancy content changes with the calcination temperature.

In this study, the magnetic properties and actual B-site vacancy content of the perovskite $\text{La}_{0.75}\text{Sr}_{0.25}\text{Mn}_{0.92}\Delta_{0.08}\text{O}_{3-\delta}$ at different calcination temperatures were investigated. The actual B-site vacancy contents are 0.08, 0.01, and 0.005 after calcination at $T_{\text{cal}} = 1073, 1273, \text{ and } 1473$ K, respectively, according to a Rietveld powder diffraction profile fitting technique and transmission electron microscopy (TEM) results. In addition, the Curie temperature was also studied, which is influenced by both B-site vacancies and the double-exchange interaction between Mn^{3+} and Mn^{4+} cations, according to the core–shell model.

2. Experimental details

Samples (0.06 mol) with the nominal composition $\text{La}_{0.75}\text{Sr}_{0.25}\text{Mn}_{0.92}\Delta_{0.08}\text{O}_{3-\delta}$ were prepared using the sol–gel method. La_2O_3 (7.3314 g, 99.99%), 3.1904 g of $\text{Sr}(\text{NO}_3)_2$ (99.50%), and 12.8279 mL of $\text{Mn}(\text{NO}_3)_2$ (50%) were dissolved in dilute HNO_3 solution, producing a light yellow solution. Then 58.1634 g of citric acid (99.5%) and 15.4001 mL of ethylene glycol (1.11 g/mL) were added as complexing agents to prevent precipitation of metal ions. The sol was treated at 373 K in a water bath for 12 h, and a gel was formed. Under further heating at 373 K in a drying cabinet for 12 h, the gel was developed. The gel was thermally treated at 773 and 873 K for 5 h each to completely decompose the organic precursor. Note that slow heating is an effective method to prevent inorganic volatilization during decomposition of the organic precursor and obtain the nominal composition as much as possible. The heat treatment details for calcination temperatures of 973, 1073, 1273, and 1473 K are shown in Table 1. For notational convenience, we denote the samples of $\text{La}_{0.75}\text{Sr}_{0.25}\text{Mn}_{0.92}\Delta_{0.08}\text{O}_{3-\delta}$ as $T_9, T_{10}, T_{12}, \text{ and } T_{14}$, corresponding to final calcination temperatures T_{cal} of 973, 1073, 1273, and 1473 K, respectively.

X-ray diffraction (XRD) data were collected using an X'pert Pro diffractometer (PANalytical Corporation, Netherlands) with $\text{Cu K}\alpha$ radiation in an angular range of $20^\circ \leq 2\theta \leq 120^\circ$ with a step size of 0.0167° . Phase identification and structural analysis were conducted using X'Pert HighScore Plus and FullProf Suite software. Scanning electron microscopy (SEM) images were obtained using an S-4800 scanning electron microscope. High-resolution TEM images were obtained using a field emission microscope (JEOL, JEM-2100F, 200 kV). The magnetic properties were measured using

a Quantum Design physical properties measurement system (Quantum Design Corporation, USA). The Curie temperature T_C was defined as the temperature at which $\frac{dM}{dT}$ reached the maximum value. Magnetization curves of the samples were measured under an applied magnetic field of up to 0.05 T.

3. Experimental results and discussion

3.1. XRD phase analyses

Fig. 1 shows the XRD patterns of the $\text{La}_{0.75}\text{Sr}_{0.25}\text{Mn}_{0.92}\Delta_{0.08}\text{O}_{3-\delta}$ samples after calcination at 973, 1073, 1273, and 1473 K. All the samples obviously have perovskite as the main phase, with space group $R\bar{3}C$. Only sample T_{10} has a single phase. T_9 has a second phase of I_4/MMM La_2CO_5 , and T_{12} and T_{14} have a second phase of La_2O_3 . The main diffraction peaks of the La_2CO_5 ($Im\bar{3}m$ space group) and La_2O_3 ($P321$ space group) phases are indicated by \nearrow and \downarrow , respectively. Because of the detection precision limit of XRD, the XRD patterns indicate that sample T_{12} , like T_{10} , has a single phase; however, sample T_{12} actually has two phases, as shown in Section 3.3. The sample calcined at 973 K has a carbon oxide, La_2CO_5 , which is not a target compound.

3.2. TEM observations of B-site vacancies

To relate the calcination temperature directly to the B-site vacancies, TEM images of samples $T_9, T_{10}, \text{ and } T_{12}$ were obtained, as shown in Fig. 2, which demonstrates that B-site vacancies (red circles) can be observed. In addition, the number of pixels of B-site vacancies for sample T_9 is larger than that for sample T_{10} , and B-site vacancies cannot be easily found for sample T_{12} , which indicates that the B-site vacancy content decreased with increasing calcination temperature.

3.3. B-site vacancy content obtained by Rietveld powder diffraction profile fitting

For the samples with the nominal composition $\text{La}_{0.75}\text{Sr}_{0.25}\text{Mn}_{0.92}\Delta_{0.08}\text{O}_{3-\delta}$, the molar content ratio of A site ions (La, Sr) to B site ions (Mn) is 1:0.92. If they form standard ABO_3 perovskite, the B-site vacancy content should be 0.08. Because the effective ion radii of La^{3+} and Sr^{2+} are larger than those of Mn^{3+}

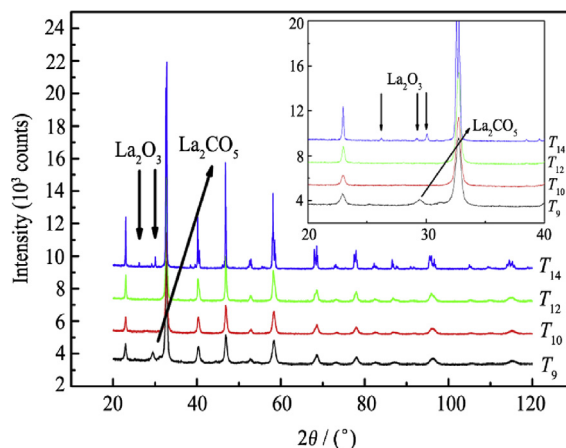


Fig. 1. XRD patterns of the samples $\text{La}_{0.75}\text{Sr}_{0.25}\text{Mn}_{0.92}\Delta_{0.08}\text{O}_{3-\delta}$ with the highest calcination temperatures 973, 1073, 1273 and 1473 K, corresponding to T_9, T_{10}, T_{12} and T_{14} , respectively. The inset shows the main diffraction peaks of the La_2O_3 or La_2CO_5 phase, marked by the symbol “ \downarrow ” or “ \nearrow ”. Other higher peaks belong to the perovskite phase.

Table 1

After calcined at 873 K, the numbers of four samples calcined with one time, two times, three times and four times. All the calcined time is 10 h.

No.	T_{cal} (K)	Times
T_9	973	1
T_{10}	973, 1073	2
T_{12}	973, 1073, 1273	3
T_{14}	973, 1073, 1273, 1473	4

Download English Version:

<https://daneshyari.com/en/article/7696909>

Download Persian Version:

<https://daneshyari.com/article/7696909>

[Daneshyari.com](https://daneshyari.com)